Journal of Advanced Mechanical Design, Systems, and Manufacturing

Vol.2, No.1, 2008

Robust Topology Optimization for Compliant Mechanisms Considering Uncertainty of Applied Loads*

Nozomu KOGISO**, WonJin AHN***, Shinji NISHIWAKI†, Kazuhiro IZUI† and Masataka YOSHIMURA†

** Department of Aerospace Engineering, Osaka Prefecture University
1-1 Gakuen-Cho, Naka-ku, Sakai, 599-8531 Japan
E-mail: kogiso@aero.osakafu-u.ac.jp

*** Department of Engineering Physics, Kyoto University
Yoshida-Honmachi, Sakyo-ku, Kyoto, 606-8501 Japan

† Department of Aeronautics and Astronautics, Kyoto University
Yoshida-Honmachi, Sakyo-ku, Kyoto, 606-8501 Japan
E-mail: (shinji, izui, yoshimura)@prec.kyoto-u.ac.jp

Abstract

In this study, a robust topology optimization method is proposed for compliant mechanisms, where the effect that variation of the input load direction has on the output displacement is considered. Variations are evaluated through a sensitivity-based robust optimization approach, with the variance evaluated using first-order derivatives. The robust objective function is defined as a combination of maximizing the output deformation under the mean input load and minimizing variation in the output deformation as the input load is varied, where variance due to changes in load can be obtained through mutual compliance and the presence of a pseudo load. For the topology optimization, a modified homogenization design method using the continuous approximation assumption of material distribution is adopted. The validity of the proposed method is confirmed with two compliant mechanism design problems. The effect that varying the input load direction has upon the obtained configurations is investigated by comparing these with deterministic optimum topology design results.

Key words : Robust Design, Topology Optimization, Compliant Mechanism, Homogenization Method, Sensitivity-Based Robust Optimization

1. Introduction

The designs of mechanical mechanisms often employ rigid parts linked together via movable joints, and in such mechanisms, the joints constrain the relative motion of such links. In contrast, compliant mechanisms take advantage of a structure's flexibility to achieve a specified motion, exploiting the elastic deformation of a continuous material instead the movement of parts constrained by joints[(1)]. Such compliant mechanisms are made of fewer parts than conventional rigid link mechanisms and offer several advantages, such as reduced operational noise, freedom from lubrication requirements, and ease of miniaturization. The use of compliant mechanisms in mechanical products, medical instruments and MEMS (Micro-Electro Mechanical Systems) is therefore expected to become more widespread.

Since the homogenization design method (HDM)[(2)] was first proposed, topology optimization approaches have become increasingly sophisticated, and some have been applied to the configuration design of compliant mechanisms. An example of such an approach is its application to aeroelastic structural design in the conceptual design phase[(3)], and a homogenization-based topology optimization method for obtaining compliant mechanism configurations has also been proposed[(4)], where the objective function is formulated as a multi-

*Received 28 Dec., 2006 (No. 06-0337)
[DOI: 10.1299/jamdsm.2.96]

objective problem to maximize the mean compliance to achieve the specified motion, and minimize the mutual mean compliance to support reaction forces.

Topology optimization results, however, are often plagued by various numerical instability problems that produce checkerboard patterns. Several schemes based on filtering techniques are routinely used to try and resolve such indeterminacies, but these merely address the symptoms rather than the core difficulty. However, several methods have been proposed that solve this issue theoretically, such as the method of continuous approximation of material distribution[5], and this kind of approach has been applied to the topology optimization of compliant mechanism designs whose optimal configurations avoided checkerboard patterns[6].

At the present time, product safety, reliability and robustness are increasingly important requirements in product design. Most studies in the topology optimization of compliant mechanisms have been conducted under deterministic conditions, where material properties and applied loads are not subject to variations. Such compliant mechanisms are usually designed to achieve a specified motion under a specified load, but when the actual direction of applied loads is different from the design specification, as may often occur in the field, the mechanism may fail to respond appropriately. In particular, small mechanisms such as MEMS are likely to be quite sensitive to variations in material properties, dimensions or environmental factors such as applied loads.

A robust design is one that maintains a particular insensitivity with respect to external noise or uncertainty. In this sense, a robust design approach lies in the same category as reliability-based designs that consider uncertainties based on probabilistic theory[7],[8], however robust designs do not employ strict definitions for modeling uncertainty beyond a formulation that uses the mean and variance of the performance.

Consequently, there are many variations in robust design approaches, such as the Taguchi method[9], the sensitivity-based robust optimization approach[10], the physical programming approach[11],[12], and robust design with an axiomatic approach[13]. The various advantages and disadvantages of these approaches are discussed in a review paper[14]. A further approach is offered by information gap decision theory[15], building on convex models[16] and their application to the evaluation of insensitive or worst case designs (e.g., Ref. (17)).

This study proposes a robust topology optimization method for compliant mechanism design that considers the effect of uncertainty in applied loads, and adopts a sensitivity-based robust optimization approach because of its suitability for continuous optimization problems and applicability to large-scale problems that have many design variables. Additionally, the sensitivity-based optimization approach requires minimal parameter settings. On the other hand, the physical programming approach and robust design method with axiomatic approach are suitable for investigating the effects of several kinds of uncertainties, however, since this study only considers the variation of applied loads, none of these approaches are adopted. The convex model approach is another candidate, but it is not well suited to the investigation of variations in structural response due to variation in applied loads because the obtained results depend on how the convex set is defined when describing uncertainties.

The robust optimal configurations of compliant mechanisms are obtained by the proposed method that combines a sensitivity-based robust optimization approach with topology optimization. Numerical examples are provided to investigate how variation in input load direction affects the output deformation of the obtained optimal compliant mechanism configurations.

The rest of this paper is organized as follows. Section 2 describes the topology optimization of the compliant mechanism design method. Section 3 describes the formulation for achieving robust designs, using the sensitivity-based robust optimization approach. To demonstrate the effectiveness of the proposed method, it is applied to two compliant mechanism design examples, as described in section 4, and section 5 provides a summary of the results.

2. Compliant mechanism design using topology optimization

Consider the design problem of determining the boundary of the design domain Ω_d by minimizing or maximizing objective functions. The key idea of the topology optimization method is the introduction of a fixed, extended design domain D that includes the prescribed original design domain Ω_d, and the utilization of the following characteristic function[18].

$$\chi_\Omega(\boldsymbol{x}) = \begin{cases} 1 & (\text{if } \boldsymbol{x} \in \Omega_d) \\ 0 & (\text{if } \boldsymbol{x} \in D \backslash \Omega_d) \end{cases} \tag{1}$$

where $\boldsymbol{x}$ denotes a position in the extended design domain D. Using this function, the original structural design problem is replaced by a material distribution problem incorporating an elasticity tensor, $\chi_\Omega \boldsymbol{E}$, in the extended design domain D, where $\boldsymbol{E}$ is the elasticity tensor in the original design domain Ω_d. Since this characteristic function can be very discontinuous, i.e., resides in $L^\infty(D)$, some regularization or smoothing technique is required in the numerical treatment. The homogenization method[2] is used to relax the solution space by introducing microstructures representing the composite materials. The design variables, however, are approximated by piecewise constants in the finite element implementation, which often leads to numerical instabilities such as checkerboard patterns.

Two types of methods have been proposed to regularize the design domain: The HDM (Homogenization Design Method)[2),(19)] and the SIMP (Solid Isotropic Material with Penalization) method[20]. In the HDM, a homogenization method is used to perform the relaxation of the solution space, by introducing microstructures that represent the composite materials. The SIMP method simply uses a fictitious isotropic material whose elasticity tensor is assumed to be a function of penalized material density expressed by an exponent parameter. Design variables are approximated by piecewise constants in the finite element implementation in both the HDM and the SIMP method even though the material density is assumed to be continuously distributed almost everywhere in the extended design domain D. However, we conjecture that there are inconsistencies in these procedures, i.e., the assumption of continuous material distributions and the piecewise distribution of design variables, and that the approximations based on the use of a piecewise constant in each element cause the numerical instability problems that are manifested as checkerboard patterns.

To overcome such obstacles and maintain procedural consistency here, the discretized design variables are not allocated at the elements' center, but at their nodes, and continuous material distributions are assumed using a continuous interpolation function at each node[5]. That is, the design variable $r(\boldsymbol{x})$ is approximated as follows.

$$r(\boldsymbol{x}) \approx r^h(\boldsymbol{x}) = \boldsymbol{N}^r(\boldsymbol{x})\boldsymbol{R} = \sum_{i=1}^{n} N_i^r(\boldsymbol{x}) R_i \tag{2}$$

where h stands for the discretized quantity using the FEM, $\boldsymbol{N}^h$ is a vector whose components are $N_i^r(\boldsymbol{x})$ $(i = 1, \ldots, n)$, $\boldsymbol{R}$ is a vector of nodal (discrete) design variables R_i $(i = 1, \ldots, n)$, and n is the total number of nodes, which is also the same as the number of design variables in this formulation[5].

Using the above approximation, the design variables can hold the C^0-continuity over the domain due to the partition-of-unity of $N_i^r(\boldsymbol{x})$, and they are continuously distributed in and throughout the elements. The bi-linear interpolation function is used here for $N_i^r(\boldsymbol{x})$ in the case of four-node quadrilateral elements, for its simplicity in this research and because it preserves the C^0-continuity. Note that $N_i^r(\boldsymbol{x})$ $(i = 1, \ldots, n)$ are selected and evaluated independently of the shape functions for displacement fields. Also note that similar formulations based on the SIMP method were presented in Refs. (21) and (22). Although they pointed out some numerical problems such as "layering" and "islanding" when using coarse meshes, the numerical examples obtained by the method proposed here will show clear optimal configurations given sufficiently fine meshes, without the above problems.

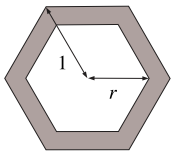

Fig. 1 Microstructure used for the design domain relaxation

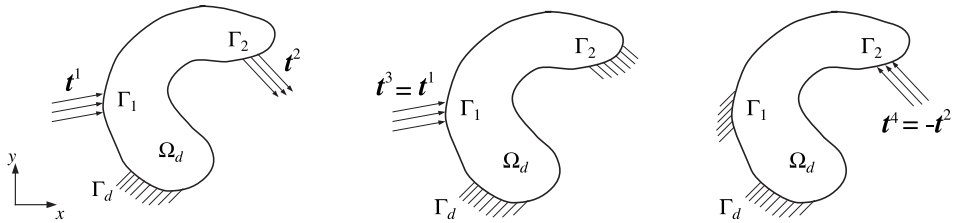

Fig. 2 Design specifications for a compliant mechanism design

Figure 1 shows the microstructure used for the relaxation of the design domain in the two-dimensional problem. As shown in this figure, its shape is hexagonal and the design variable is a geometrical parameter r. In order for a unit cell to be void, r must be 1, and for it to be solid material, r must be 0. This microstructure has an isotropic response. Using this microstructure, whose elasticity tensor is $\boldsymbol{E}$, the homogenized elasticity tensor $\boldsymbol{E}^H$ is calculated as,

$$\boldsymbol{E}^H = \frac{1}{|Y|}\int_Y \boldsymbol{E}(x,y)\left[\boldsymbol{I} - \boldsymbol{\epsilon}_y(\boldsymbol{\chi})\right]\, dY \tag{3}$$

where $\boldsymbol{\chi}$ indicates the characteristic deformations obtained by the following equation:

$$\int_Y \boldsymbol{\epsilon}_y(\boldsymbol{v})^T \boldsymbol{E}(x,y)\boldsymbol{\epsilon}_y(\boldsymbol{\chi}(x,y))\, dY = \int_Y \boldsymbol{\epsilon}_y(\boldsymbol{v})^T \boldsymbol{E}(x,y)\, dY \qquad \text{for } \forall \boldsymbol{v} \in V_y \tag{4}$$

$$\boldsymbol{\epsilon}_y(\boldsymbol{v})^T = \left(\frac{\partial v_1}{\partial y_1} \quad \frac{\partial v_2}{\partial y_2} \quad \frac{1}{2}\left(\frac{\partial v_1}{\partial y_2} + \frac{\partial v_2}{\partial y_1}\right)\right) \tag{5}$$

and $\boldsymbol{y}$ is the local coordinate defined in the microstructure, and V_y is the admissible space defined in unit cell Y such that

$$V_y = \{\boldsymbol{v} = v_i \boldsymbol{e}_i : \quad Y\text{-periodic in unit cell } Y\} \tag{6}$$

where $|Y|$ stands for the area of the unit cell. We thus obtain the homogenized properties that are then utilized in the optimization procedure.

Next, let us consider that the original design domain for a compliant mechanism, Ω_d, is fixed at boundary Γ_d, and is subjected to an applied traction $\boldsymbol{t}^1$ at boundary Γ_1 as shown in Figure 2 (a). We also consider an extended design domain D that includes Ω_d. We intend to design a compliant mechanism that starts to deform in the specified direction $\boldsymbol{t}^2$ at boundary Γ_2 in order to carry out its intended design function when a traction $\boldsymbol{t}^1$ is applied at boundary Γ_1. To successfully implement this function in the compliant mechanism, kinematic and structural requirements must be satisfied simultaneously. For the kinematic requirement, the compliant mechanism must have sufficient flexibility to allow appropriate deformation along a direction specified by a dummy load $\boldsymbol{t}^2$ at Γ_2 when traction $\boldsymbol{t}^1$ is applied at Γ_1 as shown in Figure 2 (a). This is obtained by maximizing the mutual mean compliance formulated by

$$l^2\left(\boldsymbol{u}^1\right) = \int_{\Gamma_2} \boldsymbol{t}^2 \cdot \boldsymbol{u}^1\, d\Gamma \qquad \boldsymbol{u}^1 \in V^1, \tag{7}$$

where

$$V^1 = \{\boldsymbol{v} = v_i \boldsymbol{e}_i : \quad \boldsymbol{v} = 0 \text{ on } \Gamma_d\} \tag{8}$$

Note that the deformation of the compliant mechanism may be considerable, but the effect of large deformations can be ignored in the topology design phase. That is, the compliant mechanism is designed based on a small linear deformation assumption since the goal is for it to qualitatively deform in the desired direction of motion. It is not necessary to consider utilizing any additional functions based on non-linear effects such as buckling at this phase of the design process. This assumption is appropriate when the qualitative characteristics of the mechanism is considered in the compliant mechanism design.

Concerning structural requirements, the compliant mechanism must have sufficient stiffness in appropriate locations in order to form a durable structure, even though the primary goal is to implement sufficient flexibility in the structure. Two different kinds of stiffness at two different boundaries are considered. One aims to provide sufficient stiffness at boundary Γ_1 as shown in Figure 2 (b) when traction $\boldsymbol{t}^1$ is applied at boundary Γ_1, which maintains the overall shape of the compliant mechanism when it deforms due to traction $\boldsymbol{t}^1$. This property is obtained by minimizing the mean compliance at boundary Γ_1 in response to traction $\boldsymbol{t}^3 = \boldsymbol{t}^1$ while boundary Γ_2 is fixed, as follows:

$$l^3\left(\boldsymbol{u}^3\right) = \int_{\Gamma_1} \boldsymbol{t}^3 \cdot \boldsymbol{u}^3 \, d\Gamma \qquad \boldsymbol{u}^3 \in V^3, \tag{9}$$

where

$$V^3 = \{\boldsymbol{v} = v_i \boldsymbol{e}_i : \quad \boldsymbol{v} = 0 \text{ on } \Gamma_d \text{ and } \Gamma_2\} \tag{10}$$

The other required stiffness is at boundary Γ_2 as shown in Figure 2 (c), which maintains the shape of the compliant mechanism against the reaction force imposed from the workpiece contacted. Here, the direction of the reaction force is assumed to be opposite to that of the dummy load $\boldsymbol{t}^3$ and it is obtained by minimizing the mean compliance at boundary Γ_2 in response to traction $\boldsymbol{t}^4 = -\boldsymbol{t}^2$ while boundary Γ_1 is fixed, as follows:

$$l^4\left(\boldsymbol{u}^4\right) = \int_{\Gamma_2} \boldsymbol{t}^4 \cdot \boldsymbol{u}^4 \, d\Gamma \qquad \boldsymbol{u}^4 \in V^4, \tag{11}$$

where

$$V^4 = \{\boldsymbol{v} = v_i \boldsymbol{e}_i : \quad \boldsymbol{v} = 0 \text{ on } \Gamma_d \text{ and } \Gamma_1\} \tag{12}$$

Note that these fixed conditions theoretically provide the compliant mechanism with over constraints because the reciprocal theorem requires a constraint only in the direction along which the traction is applied in the pseudo or quasi-static case. However, as a matter of practicality, we impose fixed conditions instead of the exact boundary conditions mentioned above, because the direction of the traction applied to the complaint mechanism keeps changing as the complaint mechanism deforms. That is, if we consider the exact boundary conditions, they might not provide the complaint mechanism with sufficient flexibility because the direction along which the traction is applied changes as the compliant mechanism deforms. Thus, boundary conditions are set in order to obtain sufficient stiffness in both cases.

To obtain the optimal configuration of a compliant mechanism here, three objective functions must be implemented, namely, to maximize Eq. (7) and to minimize Eqs. (9) and (11). In order to incorporate the three objective functions, the objective function is converted to the single objective function. The optimization problem is formulated to use this single objective function under a volume constraint.

$$\text{maximize :} \quad f = \frac{l^2(\boldsymbol{u}^1)}{w_3 l^3\left(\boldsymbol{u}^3\right) + w_4 l^4\left(\boldsymbol{u}^4\right)} \tag{13}$$

$$\text{subject to :} \quad V(\boldsymbol{x}) \leq V_U \tag{14}$$

where w_3 and w_4 are weighting coefficients and V_U is the volume upper constraint. See the details in Ref. (4).

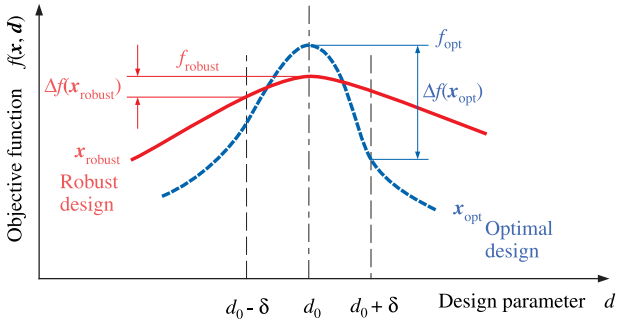

Fig. 3 Concept of robust optimization.

This formulation is based on a conventional deterministic optimization problem. In order to obtain an optimal configuration of a robust compliant mechanism where variation in applied load is considered, measures to evaluate robustness should be introduced into the objective function.

3. Formulation of robust objective function

A sensitivity-based robust optimization approach[10] is used in this study because of its suitability when applied to continuous optimization problems. In this method, the robustness of the objective function is usually described as a weighted sum of the mean objective value and variation of the objective with respect to the variations of design variables and design parameters. This can be defined by using the mean value $E[\cdot]$ and variance $\mathrm{Var}[\cdot]$ as follows.

$$\text{maximize}: \quad F(\boldsymbol{x}) = E[f(\boldsymbol{x}, \boldsymbol{d})] - \alpha \mathrm{Var}[f(\boldsymbol{x}, \boldsymbol{d})] \tag{15}$$

where $\boldsymbol{x}$ and $\boldsymbol{d}$ indicate design variables and design parameters, respectively, and α is a positive weighting coefficient. This objective function combines a maximization of the mean performance with a minimization of variations due to uncertainty and is illustrated conceptually in Figure 3. The deterministic optimum solution $\boldsymbol{x}_{\mathrm{opt}}$ shows a larger variation of the objective $\Delta f(\boldsymbol{x}_{\mathrm{opt}})$ in response to a specified change δ in the design parameters, whereas the robust optimum solution yield a smaller corresponding variation $\Delta f(\boldsymbol{x}_{\mathrm{robust}})$ even when the objective function of the robust design f_{robust} is smaller than that of the optimum design f_{opt}.

For the robust constraint conditions, certain constraints are satisfied within the variable range for the design variables and design parameters. That is, the j-th constraint condition is modified as follows.

$$g_j(E[\boldsymbol{x}] + \boldsymbol{z}^x, E[\boldsymbol{d}] + \boldsymbol{z}^d) \leq 0 \tag{16}$$

where $\boldsymbol{z}^x$ and $\boldsymbol{z}^p$ indicate variable ranges of design variables and design parameters, respectively. The other constraints are formulated in the same manner used for conventional deterministic optimization problems.

The mean and variance of the objective function f are evaluated according to the following first-order approximation.

$$E[f] \approx f(E[\boldsymbol{x}], E[\boldsymbol{d}]), \tag{17}$$

$$\mathrm{Var}[f] \approx \sum_{i=1}^{n_x} \left(\frac{\partial f}{\partial x_i} \right)^2 \mathrm{Var}[x_i] + \sum_{i=1}^{n_d} \left(\frac{\partial f}{\partial d_i} \right)^2 \mathrm{Var}[d_i] \tag{18}$$

where, n_x and n_d are the number of design variables and uncertain parameters, respectively.

The first order approximation does not always have sufficient accuracy because the derivative indicates only the change within an infinitely small range, and in particular, because the derivative with respect to a design variable would become zero at the deterministic optimum

value. Sundaresan *et al.*[10] proposed that the variance be approximated by the mean square sum of the difference between the objective function value at current design points f_i and at the central point f_c, and this is called a sensitivity index.

$$\mathrm{Var}[f] \approx \frac{1}{n_x}\sum_{i=1}^{n_x}(f_i - f_c)^2 \tag{19}$$

In any case, this approximation imposes a disproportionately large computational cost in comparison with the derivative approach. The derivative approach provided in Eq. (18) is thus a better strategy for case where there is a relatively small range of variations[23].

In this study, the applied input load is assumed to have variation, while the design variables corresponding to the topology are specified as being deterministic. In this case, changes in the objective function with respect to design parameters, not design variables, are considered to be confirmed to a relatively small range of variation. However, even at its smallest, a derivative with respect to a design parameter would not become zero at the deterministic optimum, which is why the variance here is formulated using a derivative approach in Eq. (18).

When the input load direction is varied, only the mutual mean compliance $l^2(\boldsymbol{u}^1)$ in Eq. (7) is affected. Therefore, the robust objective function is formulated to maximize the mutual mean compliance and minimize the variation as follows.

$$\text{maximize}: \quad F = \frac{E[l^2(\boldsymbol{u}^1)] - \alpha\sqrt{\mathrm{Var}[l^2(\boldsymbol{u}^1)]}}{w_3 l^3(\boldsymbol{u}^3) + w_4 l^4(\boldsymbol{u}^4)} \tag{20}$$

where the standard deviation is used instead of the variance to set the same dimension as the first term of the numerator and α is a positive weighting coefficient.

Variation of the input load direction is modeled by introducing an uncertain traction $\boldsymbol{t}_r^1$ whose direction is perpendicular to the input load $\bar{\boldsymbol{t}}^1$ as shown in Figure 4. That is,

$$\boldsymbol{t}^1 = \bar{\boldsymbol{t}}^1 + \boldsymbol{t}_r^1, \tag{21}$$

$$\boldsymbol{t}_r^1 \cdot \bar{\boldsymbol{t}}^1 = 0 \tag{22}$$

the input load $\bar{\boldsymbol{t}}^1$ is assumed to be deterministic and the average of variable traction $\bar{\boldsymbol{t}}^1$ is set to zero, so that

$$E[\boldsymbol{t}^1] = \bar{\boldsymbol{t}}^1, \qquad \mathrm{Var}[\bar{\boldsymbol{t}}^1] = 0, \tag{23}$$

$$E[\boldsymbol{t}_r^1] = 0, \qquad \mathrm{Var}[\boldsymbol{t}_r^1] = \boldsymbol{\sigma}_{t^1}^2 \tag{24}$$

Under this assumption, the average and variance of the mutual mean compliance in Eq. (20) are described as follows.

$$E[l^2(\boldsymbol{u}^1)] = l^2(\bar{\boldsymbol{u}}^1), \tag{25}$$

$$\mathrm{Var}[l^2(\boldsymbol{u}^1)] = \left(\boldsymbol{\sigma}_{t^1} \cdot \frac{\partial l^2(\boldsymbol{u}^1)}{\partial \boldsymbol{t}_1^r}\right)^2 \tag{26}$$

where $\bar{\boldsymbol{u}}^1$ is the deformation due to the average traction $\bar{\boldsymbol{t}}^1$. Variation of Eq. (26) is obtained by the first Taylor series under the assumption that variation in the output deformation is relatively small.

The derivative of the mutual mean compliance $l^2(\boldsymbol{u}^1)$ with respect to the variable traction $\boldsymbol{t}_r^1$ is described as follows.

$$\frac{\partial l^2(\boldsymbol{u}^1)}{\partial \boldsymbol{t}_1^r} = \boldsymbol{u}_r^1 \tag{27}$$

where $\boldsymbol{u}_r^1$ is the variation in deformation at the input point due to variation of the input load $\boldsymbol{t}_r^1$. Additionally, the direction of the variable deformation $\boldsymbol{u}_r^1$ can be assumed to be coincident

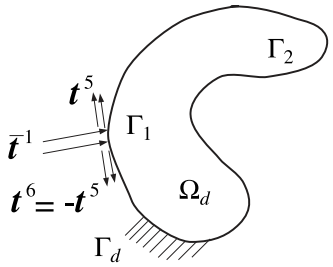

Fig. 4 Modeling of variable load direction.

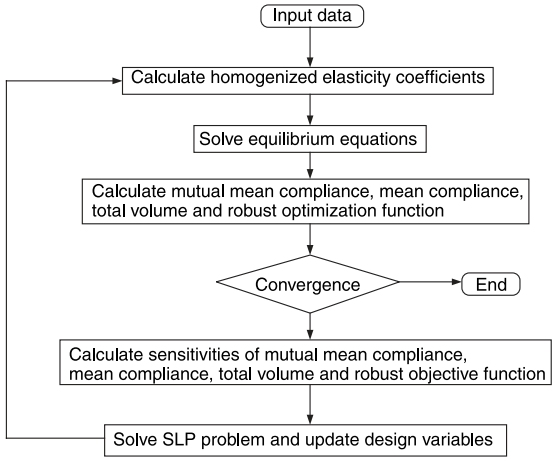

Fig. 5 Flowchart of robust topology optimization procedure.

with the direction of the variable load $\boldsymbol{\sigma}_{t^1}$ that is defined as being perpendicular to the average load in Eq. (21). Consequently, Eq.(26) yields the following scalar product.

$$\mathrm{Var}[l^2(\boldsymbol{u}^1)] = \left(|\boldsymbol{\sigma}_{t^1}| \cdot |\boldsymbol{u}_r^1|\right)^2 = (\sigma_{t^1} u_r^1)^2 \tag{28}$$

The variable deformation $\boldsymbol{u}_1^r$ is obtained by the average of mean compliance due to unit pseudo loads in both directions along $\boldsymbol{t}_r^1$ as follows.

$$\boldsymbol{u}_r^1 = \frac{l^5(\boldsymbol{u}^5) + l^6(\boldsymbol{u}^6)}{2} \tag{29}$$

$$l^5(\boldsymbol{u}^5) = \int_{\Gamma_1} \boldsymbol{t}^5 \cdot \boldsymbol{u}^5 \, d\Gamma, \qquad \boldsymbol{u}^5 \in V^5, \tag{30}$$

where

$$V^5 = \{\boldsymbol{v} = v_i \boldsymbol{e}_i : \ \boldsymbol{v} = 0 \text{ on } \Gamma_d\} \tag{31}$$

$$l^6(\boldsymbol{u}^6) = \int_{\Gamma_1} \boldsymbol{t}^6 \cdot \boldsymbol{u}^6 \, d\Gamma, \qquad \boldsymbol{u}^6 \in V^6, \tag{32}$$

where

$$V^6 = \{\boldsymbol{v} = v_i \boldsymbol{e}_i : \ \boldsymbol{v} = 0 \text{ on } \Gamma_d\} \tag{33}$$

where the unit pseudo loads are described as $\boldsymbol{t}^5$ and $\boldsymbol{t}^6$ having opposite directions, respectively, as shown in Figure 4.

The robust optimization problem is formulated as follows.

$$\text{maximize :} \quad F = \frac{l^2(\boldsymbol{u}^1) - \alpha' \left[\sigma_{t^1} \left\{l^5(\boldsymbol{u}^5) + l^6(\boldsymbol{u}^6)\right\}\right]}{w_3 l^3(\boldsymbol{u}^3) + w_4 l^4(\boldsymbol{u}^4)} \tag{34}$$

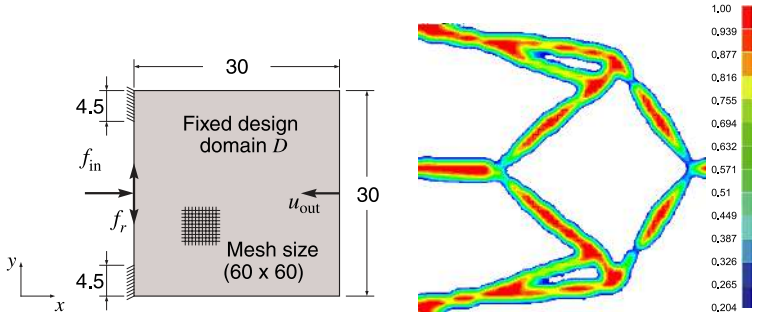

(a) Design domain. (b) Deterministic

(c) $\sigma = 0.05$ (d) $\sigma = 0.125$ (e) $\sigma = 0.25$

Fig. 6 Design domain and robust optimum configurations of example 1.

$$\text{subject to :} \quad V(\boldsymbol{x}) \leq V_U \tag{35}$$

where the parameter α' is equal to $\alpha/2$. The constraint condition is a volume constraint, which is invariable because the design variables are deterministic.

A flowchart of the topology optimization procedure is illustrated in Figure 5. As shown the homogenized coefficients for the elasticity tensor are calculated first. Next, the four equilibrium equations are solved using the finite element method. The mutual mean compliance, the mean compliance, the total volume constraint, and the robust objective function are then all computed. If the objective function converges, the procedure terminates, otherwise the sensitivities of the mutual mean compliance, the mean compliance, the total volume constraint, and the robust objective function are all computed. The design variables are then updated using sequential linear programming, and the procedure returns to the first step.

4. Numerical examples

The validity of the proposed method is demonstrated by the following two compliant mechanism design problems. The optimal configuration of robust compliant mechanism is obtained by minimizing the objective function of Eq. (34) under a volume constraint of 20% in whole design domain. Additionally, the denominator parameter values in Eq. (34) are set to $w_3 = w_4 = 1$. In order to investigate the effect of variations, the standard deviation of the input load is changed while the numerator in Eq. (34) is set to $\alpha = 1$.

4.1. Example 1 : Simple compliant mechanism

The design problem is shown in Figure 6 (a) where boundary conditions and specifications are as indicated. Consider a compliant mechanism that undergoes a horizontal deformation u_{out} in the left direction ($-x$ direction) at the central node of the right edge in response to a horizontal input load f_{in} along the right direction ($+x$ direction) applied at the central node of the left edge, where the 9 nodes at the top and bottom of the left edge are fixed. The fixed design domain D, a 30×30 square, is discretized to 60×60 square-shaped finite elements. The uncertainty of the applied load is described as the uncertain vertical load value f_r (in $\pm y$ direction) at the central node at the left edge, where the average value is set to zero and the

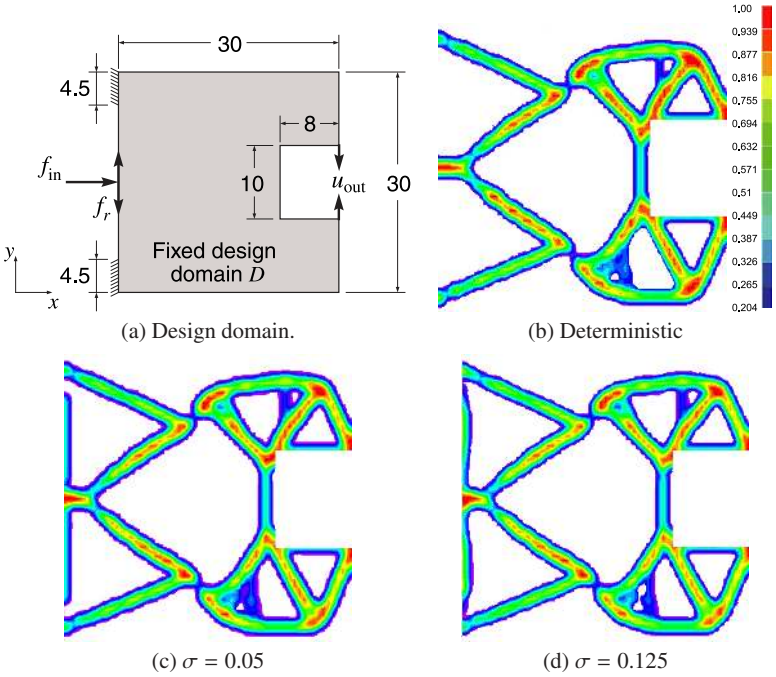

(a) Design domain. (b) Deterministic

(c) σ = 0.05 (d) σ = 0.125

Fig. 7 Design domain and robust optimum configurations of example 2.

standard deviation is in the range of 0.05 ~ 0.25.

The optimal configurations obtained with different standard deviation values are illustrated in Figure 6 (b)~(e). The obtained optimum solution is distiguished by its configuration that includes dimensions and shapes of the structural elements as well as the topology[2),(4)]. The color indicates the value of the normalized density calculated by $1 - r(\boldsymbol{x})^2$, where the red color corresponds to the highest value and the blue color to the lower. The allocated value to each color is illustrated in Figure 6 (b). Note that checker-board patterns are not observed in the optimal configurations, since the node-based continuous approximation of material distribution approach[(5)] as described in Eq. (2) is employed in the proposed method.

Figure 6 (b) shows the deterministic design that has no variations. The robust designs reveal different configurations in comparison with the deterministic design, notably in the vertical members added at the left side that support vertical input loads. The number of members is increased in the case where σ = 0.25 shown in Figure 6 (e) at the right, probably because this increases vertical stiffness to accommodate the variable vertical load.

4.2. Example 2 : Compliant gripper

The next example is a compliant gripper whose fixed design domain D is illustrated in Figure 7 (a) where boundary conditions and specifications are as indicated. The top and bottom edges at the left side are fixed to support the gripper. The function of the gripper mechanism is to deform the right hollow along the directions of u_{out} ($\pm y$ directions) in order to hold an object securely, when a horizontal input load f_{in} ($+x$ direction) is applied at the central node of the left edge. The fixed design domain D is discretized in the same size of into square finite elements as for in the previous example.

The obtained optimum configurations are illustrated in Figure 7 (b)~ (d), and Figure 7 (b) shows a deterministic design without variations where the color indicates the level of the material density as illustrated in Figure 7 (b). The difference of the topology between the robust designs is small except for the material distribution along the left edge.

To investigate the effect that the input load direction has on the output deformation, variations of the deterministic objective function value in Eq. (13) are investigated for the optimum configurations under oblique input loadings. The result is shown in Figure 8. The horizontal

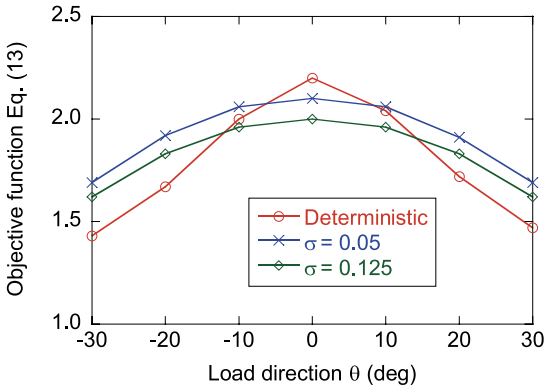

Fig. 8 Variations of objective function value.

axis denotes the direction angle of the resultant load. The deterministic design has the highest value under the deterministic condition where $\theta = 0°$, but deteriorates the performance under the oblique input loadings. While, the optimal configuration in case where $\sigma = 0.05$ has the largest values under oblique input loading. This result implies that the obtained configuration representating dimension and shape of appeared structural elements rather than the topology in this case achieves robustness with respect to the input load directions.

On the other hand, the optimal configuration in case where $\sigma = 0.125$ has smaller value than that in case where $\sigma = 0.05$, though the design has larger value than that of the deterministic design under larger angles of the load direction. The design might have larger objective function value for much larger angle of the resultant load. Such a loading condition, however, might be beyond the assumed load variance. This result indicates the difficulty of the variance value setting for the robust optimization. The adequate setting of the variance remains as one of future problems of the robust optimization.

5. Conclusion

This study proposed a robust topology optimization method for design of compliant mechanisms subject to variations in input load direction, as a first step to establish a robust design procedure for compliant mechanisms that must endure considerable variations in actual working environments.

The following conclusions were obtained.

- Based on the sensitivity-based robust optimization concept, the objective function was formulated to maximize the average value and to minimize the variance for the compliant mechanism.
- Variation in the output deformation due to variation in the direction of the input load was evaluated through the mutual mean compliance and introducing a variable input load perpendicular to the mean load direction.
- The utility of the proposed method was demonstrated with two numerical examples. In comparison with deterministic optimal configurations, robust optimal configurations show increased output deformations in response to the average applied load, and also an increased stiffness in uncertain load directions that reduces the variance of the output deformation.
- Numerical results also indicate the difficulty of setting the variance value for the robust optimization. This remains as one of future problems.

The authors hope to conduct future research that further develops the proposed method so that consideration of other variations can be included, for example in material properties, input loading positions or other environmental conditions, to establish a robust optimization method for the design of increasingly versatile compliant mechanisms.

Acknowledgement

The authors would like to express our aknowledgement to Mr. Kiyoshi Yokota, Graduate

Student of Kyoto University, of his dedicated effort on several numerical calculations.

References

(1) Howell, L. L., Compliant Mechanism, John Wiley & Sons, Inc., (2001)
(2) Bendsøe, M. P. and Kikuchi, N., Generating optimal topologies in structural design using a homogenization method, Comput. Methods. Appl. Mech. Engrg., Vol. 71 (1988), pp. 197-224.
(3) Maute, K., and Allen, M., Conceptual design of aeroelastic structures by topology optimization, Struct. Multidisc. Optim., Vol. 27 (2004), pp. 27-42.
(4) Nishiwaki, S. Min, S., Yoo, J. and Kikuchi, N., Optimal structural design considering flexibility, Comput. Methods Appl. Mech. Engrg., Vol. 190 (2001), pp. 4457-4504.
(5) Matsui, K., and Terada, K., Continuous approximation of material distribution for topology optimization, Int. J. Numer. Methods in Engrg, Vol. 59 (2004), pp. 1925-1944.
(6) M. Kobayashi, S. Nishiwaki, K. Izui and M. Yoshimura, An innovative design method for compliant mechanisms combining structural optimizations and designer creativity, Journal of Engineering Design, (*To appear, Online, 19 sep. 2007*)
(7) Thoft-Christensen, P., and Murotsu, Y., Application of Structural Systems Reliability Theory, Springer-Verlag, (1986)
(8) Haldar, A., and Mahadevan, S., Probability, Reliability and Statistical Methods in Engineering Design, John Wiley & Sons, (2000)
(9) Phadke, M. S., Quality engineering using robust design, Prentice-Hall, (1989)
(10) Sundaresan, S., Ishii,K., and Houser, D. R., A robust optimization procedure with variations on design variables and constraints, Eng. Opt., Vol. 24, No. 2 (1995), pp. 101-117.
(11) Messac, A., Physical programming: Effective optimization for computational design, AIAA J., Vol. 34 (1996), pp. 149-158.
(12) Messac, A. and Ismail-Yahaya, A., Multiobjective robust design using physical programming, Struct. Multidisc. Optim., Vol 23 (2002), pp. 357-371.
(13) Suh, N. P., Axiomatic design: advances and applications, Oxford University Press, (2001)
(14) Park, G. J., Lee, T. H., Lee, K. H., and Hwang, K. H., Robust design: an overview, AIAA J., Vol. 44, No. 1 (2006), pp. 181-191.
(15) Ben-Haim, Y., Information gap decision theory, Decisions under severe uncertainty, Academic Press (2001).
(16) Ben-Haim, Y. and Elishakoff, I., Convex models of uncertainty in applied mechanics, Studies in applied mechanics, 25, Elsevier (1990).
(17) e.g., Fryba, L. and Yoshikawa, N., Bounds Analysis of a Beam Based on the Convex Model of Uncertain Foundation, Journal of Sound and Vibration, Vol. 212, No. 3 (1998), pp.547-557
(18) Murat, F. and Tartar, L., Optimality conditions and homogenization, *Nonlinear variational problems*, Mario A, Modica L, and Spagnolo S, (eds.), Pitman Publishing Program, (1985), pp. 1-8.
(19) Suzuki, K. and Kikuchi, N., A homogenization method for shape and topology optimization. Comput. Methods. Appl. Mech. Engrg., Vol. 93, (1991), pp. 291-318.
(20) Bendsøe, M. P. and Sigmund, O., Topology optimization theory, Methods and applications, (2003) Springer-Verlag.
(21) Rahmatalla, S. and Swan, C. C., Form finding of sparse structures with continuum topology optimization, J. Struct. Eng., Vol. 129 (2003), pp. 1707-1716.
(22) Rahmatalla, S. and Swan, C. C., A Q4/Q4 continuum structural topology optimization implementation, Struct. Multidisc. Optim., Vol. 27 (2004), pp. 130-135.
(23) Su, J. and Renaud, J. E., Automatic differentiation in robust optimization, AIAA J., Vol. 35, No. 6 (1997), pp. 1072-1079.